DESIGN AND EXPERIMENT OF IWOA-OPTIMIZED FUZZY PID VARIABLE FERTILIZATION CONTROL SYSTEM FOR RICE BASED ON N-P-K HYBRID PRESCRIPTION GRAPH

/

基于 N-P-K 融合处方图的 IWOA 优化模糊 PID 水稻变量施肥控制系统设计与试验

Kun ZHANG[1)], Lin WAN[*1,2)], Gang CHE[1,2)], Chun-sheng WU[*3)], Xi-lu LI[3)]

[1)] College of Engineering, Heilongjiang Bayi Agricultural University, Daqing 163319, China

[2)] Key Laboratory of Intelligent Agricultural Machinery Equipment in Heilongjiang Province, Daqing 163319, China

[3)] Heilongjiang Province Agricultural Machinery Science Research Institute - Jiamusi Branch, Jiamusi 154004, China

Tel:+86-459-13555523188; E-mail: 381995603@qq.com

Corresponding author: Lin Wan

Tel:+86-459-18546403666; E-mail: wcs70@163.com

Corresponding author: Chun-sheng Wu

DOI: https://doi.org/10.35633/inmateh-79-09

Keywords: *Rice, variable fertilization, three-dimensional prescription map, whale optimization algorithm, fuzzy PID control*

ABSTRACT

Traditional uniform fertilization in rice paddy fields is associated with low fertilizer-use efficiency and severe agricultural non-point source pollution. Existing variable-rate fertilization equipment commonly presents limitations such as reliance on single-source prescription information and insufficient control precision. To address these issues, this study uses an impeller-type fertilizer applicator as the working platform and, considering the characteristics of cold-region rice cultivation in Heilongjiang Province, constructs an integrated ternary nitrogen-phosphorus-potassium fertilization prescription map. A mapping model between fertilizer application rate and motor speed is established, and a fuzzy PID controller optimized using an improved whale optimization algorithm (IWOA) is designed. Fertilizer-discharge calibration tests and field trials were conducted. The results showed that the coefficient of determination (R^2) between fertilizer discharge rate and motor speed reached 0.9912. The IWOA-fuzzy PID algorithm achieved a step-response overshoot of only 3.3% and a settling time of 1.55 s, while the relative error of field fertilization was controlled within ±5%.

摘要

水稻格田传统均匀施肥模式存在肥料利用率低、农业面源污染突出等问题，现有变量施肥装备普遍存在处方信息单一和控制精度不足等缺陷。针对上述问题，本文以叶轮式施肥装置为作业载体，结合黑龙江寒地水稻种植特点，构建氮磷钾三元融合施肥处方图。建立施肥量 - 电机转速映射模型，设计基于改进鲸鱼算法（IWOA）优化的模糊 PID 控制器。开展排肥标定试验，以及田间试验。试验结果表明：排肥量与电机转速拟合决定系数 R^2=0.9912，IWOA - 模糊 PID 算法阶跃响应超调量仅 3.3%，调节时间 1.55 s，田间施肥相对误差控制在 ±5% 以内。

INTRODUCTION

The area of rice cultivation in our country is vast, and it is a pillar industry for ensuring national food security. The traditional fertilization model has led to increasingly prominent issues of resource waste and ecological problems (*Wang et al., 2024; Ren et al., 2023*). In the scenario of large-scale production of rice fields, the extensive and uniform fertilization method causes a decline in fertilizer utilization rate and an increase in agricultural non-point source pollution (*Li et al., 2022; Liu et al., 2012*). With the rapid iteration of smart agriculture and precise agricultural machinery technology, variable fertilization control in rice fields has become the mainstream direction of industry development. However, during the implementation of this technology, there are always two major challenges: the complex operation environment of paddy fields and the limited computing power of edge terminals of agricultural machinery (*Hu et al., 2023; Hu et al., 2021*).

The rice field operation environment is complex and variable, and the movement of machinery is prone to skidding and jolting. Coupled with the continuous fluctuations in field humidity and soil moisture content, it not only changes the load state of the impeller fertilizer distribution mechanism but also causes problems such as fertilizer deliquescence, caking, and blockage (*Wang et al., 2024; Ding et al., 2025*).

Various interference factors in the field can mask the operation characteristics of the fertilization mechanism, making it difficult for traditional fertilization control methods to accurately identify changes in working conditions and dynamically match the fertilizer demand in the field. This is also an important cause for the current low control accuracy of variable fertilization equipment (*Bai et al., 2022; Wang et al., 2023*).

At present, variable fertilization for rice is mainly divided into two technical routes: real-time sensing and prescription map. Both schemes have their own advantages and inherent defects (*Wang et al., 2024*). Real-time sensing fertilization relies on dynamic collection of nutrient data by field sensors, with fast decision response speed, but the sensors are prone to interference from paddy mud water and dust, resulting in poor long-term operational stability and high equipment modification costs (*Li et al., 2024*). Prescription map fertilization relies on the pre-mapped nutrient layers in the field for operations, with clear decision logic and lower hardware costs, and is also the mainstream choice in domestic rice-growing areas. However, the existing prescription maps are mostly single nutrient layers and cannot meet the agronomic requirements for coordinated fertilization of nitrogen, phosphorus, and potassium (*Ding et al., 2025; Qin et al., 2025*).

In recent years, domestic and foreign research institutions and agricultural machinery enterprises have conducted a large number of research projects on variable fertilization equipment for rice, prescription map technology, and intelligent control algorithms. The team from Huazhong Agricultural University in China developed an electrically driven side-drip fertilization device for rice, optimizing the synchronization of fertilization points (*Li et al., 2024*). Northeast Agricultural University based on Kriging interpolation method constructed a fertilization prescription map for rice, combined with neural network to optimize control parameters. Xi'an University of Science and Technology used Kalman filtering to optimize sensor data, reducing fertilization control error to 2.7% (*Li et al., 2024*). Guizhou University based on the GIS platform built a fertilization decision system to achieve spatial analysis of field nutrients (*Mou et al., 2017*). Foreign enterprises such as John Deere, Kubota, and Igus have launched complete sets of intelligent fertilization agricultural machinery, relying on high-precision positioning technology to achieve dynamic variable operations (*Abdalla & Nafchi, 2024*); several domestic agricultural technology enterprises have also introduced mass-produced variable fertilization equipment, achieving certain fertilizer-saving effects in large-field operations (*Wang et al., 2004; Chen Li et al., 2008*). These studies have advanced variable fertilization technology from different dimensions such as equipment structure, data processing, and algorithm optimization, providing a solid theoretical and practical foundation for subsequent research.

PID and fuzzy PID algorithms are the most widely used mainstream technologies in the field of agricultural mechanical control (*Wang et al., 2023*). The traditional PID algorithm has a simple structure and is easy to implement in engineering, but its parameters are fixed and have poor control effect when facing nonlinear loads of the impeller fertilizer distribution mechanism and system time delays (*Chen et al., 2008*); the basic fuzzy PID can achieve online self-adaptive adjustment of parameters, but the fuzzy rules and initial parameters are mostly set based on manual experience, which is prone to fall into local optimal solutions and easily causes excessive overshoot and lag in dynamic working conditions such as sudden changes in vehicle speed and load disturbances (*Qin et al., 2025; Bai et al., 2022*). The limitations of existing algorithms further restrict the operational accuracy and working condition adaptability of variable fertilization equipment.

MATERIALS AND METHODS

Fertilizer application device structure and working principle

The wheeled fertilizer distributor uses the separated blades of the impeller to form independent fertilizer chambers for fertilizer filling and discharge. Since the fertilizer is not forcibly squeezed during operation, problems such as particle breakage, deliquescence, adhesion, and blockage in compound fertilizers can be effectively avoided. At the same time, the continuous and smooth fertilizer-discharge process during impeller rotation ensures a good linear relationship between discharge amount and impeller speed, thereby meeting the dynamic regulation requirements of prescription-chart-based variable-rate fertilization.

The device adopts a centrifugal fertilizer application device, which consists of a fertilizer box, a centrifugal fertilizer discharger, a fertilizer discharging motor, a fan, etc. The discharge port at the bottom of the fertilizer box is connected to the fertilizer inlet of the discharger. After receiving the control instructions, the motor drives the centrifugal fertilizer wheel to rotate. Under the influence of gravity, the fertilizer particles fall into the Venturi tube. The stable air pressure output by the air system transports the fertilizer along the fertilizer guiding pipe outward. At the same time, under the action of the high-speed airflow, the fertilizer enters the mud ditch to complete the variable fertilizer application for rice.

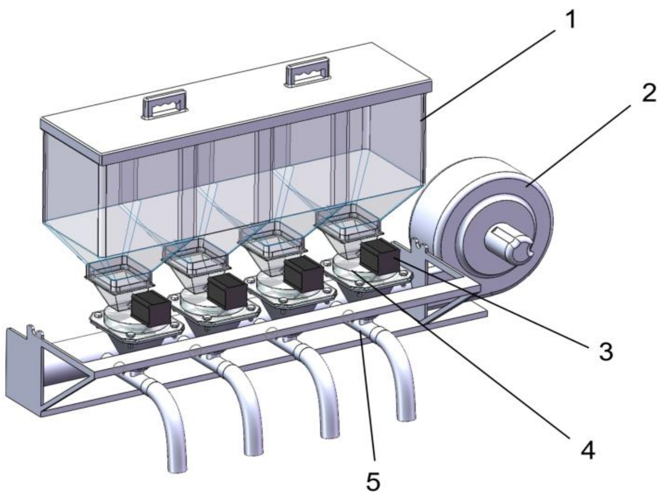

Fig. 1 - Fertilizer apparatus

1. Manure box; 2. Fan; 3.57-step motor;
4. Impeller type manure discharger; 5. Venturi tube

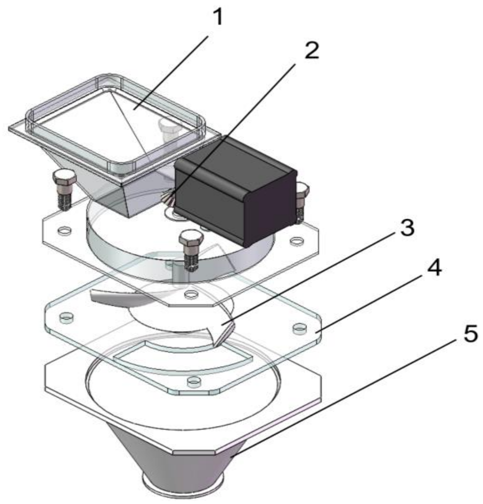

Fig. 2 - Impeller fertilizer distributor

1. Upper housing; 2. Transmission gear;
3. Impeller blade; 4. Baffle; 5. Lower housing

Overall structure and working principle of the fertilization system

A closed-loop control architecture of upper-level computer decision-making and lower-level machine execution is adopted. During the operation process, the upper-level computer matches the pre-established grid prescription map with the real-time obtained GNSS-RTK positioning information, completes spatial grid addressing based on the current position, and further calculates the target fertilization amount corresponding to the current operation position. The lower-level machine uses the ESP32 controller as the control unit. After receiving the fertilization instructions issued by the upper-level computer, it combines the real-time operation vehicle speed and converts the target fertilization amount into the theoretical rotational speed command for the fertilizer distribution motor. The lower-level machine introduces a fuzzy PID control strategy optimized based on the improved whale optimization algorithm (IWOA) to adjust the rotational speed of the fertilizer distribution motor in real time, and outputs pulse signals to drive the TB6600 stepper motor driver, thereby controlling the 57 stepper motors to complete the fertilizer distribution operation. At the same time, a Hall sensor is installed at the fertilizer distribution shaft end to collect the actual rotational speed of the motor in real time, and the feedback signal is transmitted back to the microcontroller, together with the control instructions, to form the bottom-level rotational speed closed-loop.

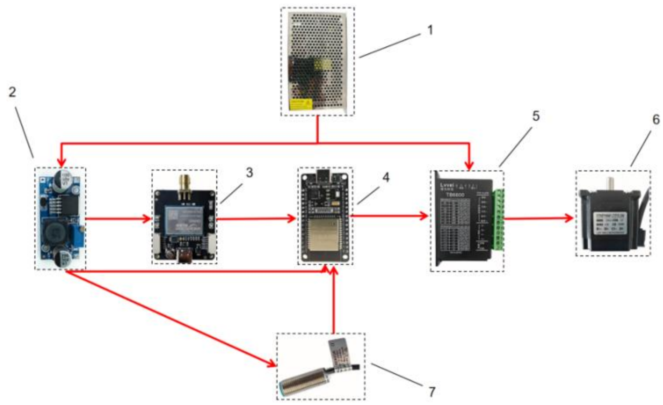

Fig. 3 - Control system hardware architecture diagram

1. 24V power supply; 2. Blood pressure reduction module; 3.RTK positioning module; 4. ESP32 microcontroller;
5. TB6600 Motor Driver; 6.57-step motor; 7. Hall sensor

CONSTRUCTION OF INTEGRATED FERTILIZATION PRESCRIPTION MAP

Nutrient spatial interpolation and rasterization

Converting the scattered and point-like vector data in the database into continuous planar control maps that the system can read is the key step in establishing the prescription map. In the ArcGIS software, rasterization processing is carried out using the ordinary Kriging spatial interpolation algorithm. Ordinary Kriging is an unbiased optimal linear estimation method and its mathematical model is shown in Eq. (1):

$$\widehat{Z}(x_0)=\sum_{i=1}^{n}\lambda_i Z(x_i) \tag{1}$$

where:

$\widehat{Z}(x_0)$ is the estimated nutrient value at the grid point x_0 that needs to be predicted, $Z(x_i)$ is the is the measured value at the known sampling point x_i, n is the number of adjacent measured points involved in the interpolation, λ_i is the weight coefficient of the i-th measured point for the predicted point.

The determination of the weight coefficient λ_i relies on the fitting of the semi-variance function, which is used to measure the spatial autocorrelation degree of soil nutrients in a certain direction and distance. The formula is expressed as follows:

$$\gamma(h)=\frac{1}{2N(h)}\sum_{i=1}^{N(h)}[Z(x_i)-Z(x_i+h)]^2 \tag{2}$$

where:

$\gamma(h)$ is the half-mutation value for a step size of h, $N(h)$ is the number of sample point pairs with a spatial distance of h.

The conventional interpolation results in a continuous gradient surface, while the actual fertilization operation is carried out based on discrete units and requires a rasterization reconstruction. Considering the 2.1-meter working width of the transplanting machine used in the experiment, the nearest neighbor method is selected for spatial resampling. The pixel scale of the prescription map is divided into 2.1m × 2.1m squares, and from a logical perspective, the geographic information is mapped into a two-dimensional control array that the microcontroller can directly read.

Calculation of target fertilizer application rate

Based on the actual operation requirements of the fertilizer application machine, practical modifications were made to the classic model. The modified model uses the absolute nutrient gap as the base, removes the low utilization compensation term that is prone to causing data fluctuations, and adds the base application ratio coefficient R.

For any grid i within the operation area, the formula for calculating the target amount of compound fertilizer to be applied based on the single-nutrient balance is as shown in Eqs. (3), (4), and (5):

$$W_{Ni}=\frac{Y\times(U_N/100)-C_{Ni}\times K_s\times E_{sN}}{F_N}\times R_N \tag{3}$$

$$W_{Fi}=\frac{Y\times(U_P/100)-C_{Pi}\times K_s\times E_{sP}}{F_P}\times R_P \tag{4}$$

$$W_{Ki}=\frac{Y\times(U_K/100)-C_{Ki}\times K_s\times E_{sK}}{F_K}\times R_K \tag{5}$$

where:

W_{Ni},W_{Fi},W_{Ki} is the theoretical amount of compound fertilizer base fertilizer calculated based on the individual requirements of nitrogen, phosphorus and potassium at grid point i for the target yield of the experimental field rice, (kg/hm^2); Y is the target yield of the rice in the experimental field, (kg/hm^2); UN, UP, UK is the amount of pure nutrients required for each 100 kilograms of rice to be formed, (kg); C_{Ni},C_{Pi},C_{Ki} is the background contents of available nitrogen, available phosphorus and available potassium obtained through kriging interpolation at grid point i, (mg/kg); K_s is the conversion constant for converting soil nutrient measurement values to the actual total nutrient content of the topsoil per hectare; E_{sN},E_{sP},E_{sK} is the seasonal utilization rate of the soil's own nutrients; F_N, F_P, F_K is the mass fraction of the corresponding effective components in the compound fertilizer; R_N,R_P,R_K is the proportion coefficients for the application of base fertilizers with different nutrient compositions.

The sampling depth for the experiment was set at the standard plough layer, which is 20 cm deep. Considering that the average bulk density of the soil in this area is approximately 1.15 g/cm³, the total weight of the plough layer soil is approximately 2.3 × 10^6 kg. Therefore, when the soil nutrient concentration is 1 mg/kg, its equivalent absolute nutrient quantity per hectare is 2.3 kg, so the constant K_s is set as 2.3.

The selected fertilizer is a controlled-release compound fertilizer. The specific N-P205-K2O ratio is 21-15-16. By dividing the formula denominator by this mass fraction, the actual nutrient requirements can be converted into the total weight of the compound fertilizer. This fertilizer contains more than 8% controlled-release fertilizer, which can effectively delay the release of nitrogen.

Table 1

Target fertilization amount calculation parameters table

Symbol	Numerical value	Units
Y	9500	kg/hm²
U_N	2.1	kg
U_P	1.1	kg
U_K	2.5	kg
F_N	0.21	%
F_P	0.15	%
F_K	0.16	%
E_{sN}	0.35	%
E_{sP}	0.4	%
E_{sK}	0.5	%
R_N	0.75	%
R_P	0.45	%
R_K	0.35	%
K_s	2.3	%

Generation of diversified and integrated prescription diagrams

The fusion weight ratio of N, P, and K was set as 0.6 : 0.3 : 0.1. On the ArcGIS software platform, the weighted overlay operation of three independent raster maps was carried out using the map algebra module. The mathematical fusion model is expressed as Eq. (6):

$$W_f(i,j)=\omega_N\cdot W_N(i,j)+\omega_P\cdot W_P(i,j)+\omega_K\cdot W_K(i,j) \tag{6}$$

where: $W_f(i,j)$ is the Integrated coordinates; Y is the target yield of the rice in the experimental field,(kg/hm^2); (i,j) is the final target amount of fertilizer application at the plot level; ω_N, ω_P, ω_K are the decision weights for nitrogen, phosphorus, and potassium; W_N, W_P, W_K calculated theoretical target quantity of the single-factor compound fertilizer.

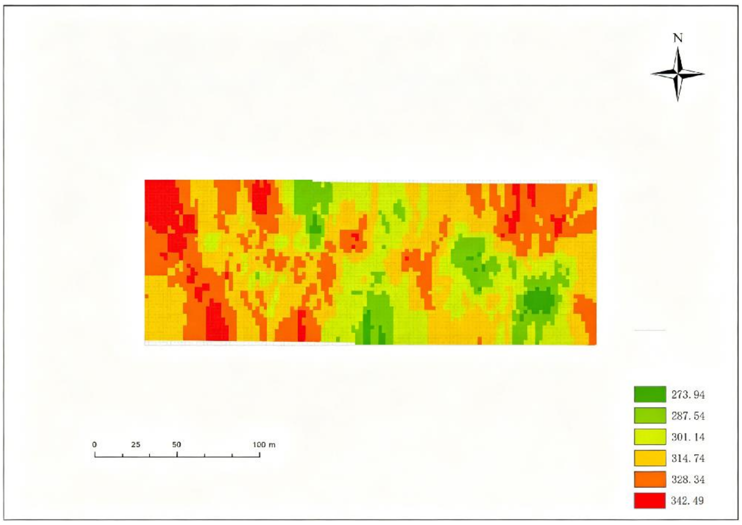

Fig. 4 - Variable fertilization integration prescription chart

IWOA - FUZZY PID ALGORITHM DESIGN

Design of fuzzy PID controller

Proportional-Integral-Derivative, abbreviated as PID, is the most widely used and mature classic algorithm in mechanical and electrical control engineering. It achieves precise regulation of the controlled object by linearly combining the error signal. The expression of PID control in continuous time is as follows:

$$u(t)=K_p\left[e(t)+\frac{1}{T_i}\int_0^t e(\tau)d\tau+T_d\frac{de(t)}{dt}\right] \tag{7}$$

where:

$u(t)$ is the controller output; $E(t)$ is the system error; Kp is the final target amount of fertilizer application at the plot level; T_i *is the integral time constant, (s);* T_d is the differentiating time constant, (s); $e(t)$ is the speed error.

If the traditional position-based PID algorithm is used directly, the program must continuously accumulate all historical rotational speed errors throughout the entire operation cycle. This not only excessively consumes the limited memory resources of the microcontroller, but the more fatal risk lies in the fact that when field operations cross the prescription map grid and the target fertilization amount instructions undergo a step-like sudden change, the accumulated massive errors will instantly trigger the integral saturation effect. Therefore, the bottom-level fertilizer application control selects the incremental digital PID control algorithm. Instead of directly outputting the absolute value of the control quantity, it outputs the incremental $\Delta u(k)$ of the control variable frequency pulse frequency. The core difference equation derivation formula is:

$$\Delta u(k)=u(k)-u(k-1) \tag{8}$$

Discretizing Eq. (7) yields the underlying running formula for the incremental PID on the microcontroller:

$$\Delta u(k)=K_p[e(k)-e(k-1)]+K_ie(k)+K_d[e(k)-2e(k-1)+e(k-2)] \tag{9}$$

where:

$K_i = K_p\frac{T}{T_i}$ is the discrete integral coefficients, $K_d=K_p\frac{T_d}{T}$ is the discrete differential coefficient.

The above incremental PID algorithm has solved the engineering implementation problems of the underlying control. However, the fixed PID parameters are difficult to adapt to complex working conditions such as load fluctuations and sudden changes in target fertilization amounts during field operations, and may lead to large control overshoot and lag in response. Therefore, this paper introduces the fuzzy control algorithm to perform online dynamic tuning of the three parameters of the PID controller. The equation is as follows:

$$\begin{cases} K_p(k)=K_{p0}+E_p\cdot\Delta K_p(k) \\ K_i(k)=K_{i0}+E_i\cdot\Delta K_i(k) \\ K_d(k)=K_{d0}+E_d\cdot\Delta K_d(k) \end{cases} \tag{10}$$

The fuzzy basic domains of the input variables e, ec and the output variables ΔK_p, ΔK_i, ΔK_d are uniformly set to the range [-3, 3]. The fuzzy domain is divided into 7 fuzzy linguistic levels, which are defined as: NB (very large negative), NM (moderately negative), NS (small negative), ZO (zero), PS (small positive), PM (moderately positive), and PB (very large positive).

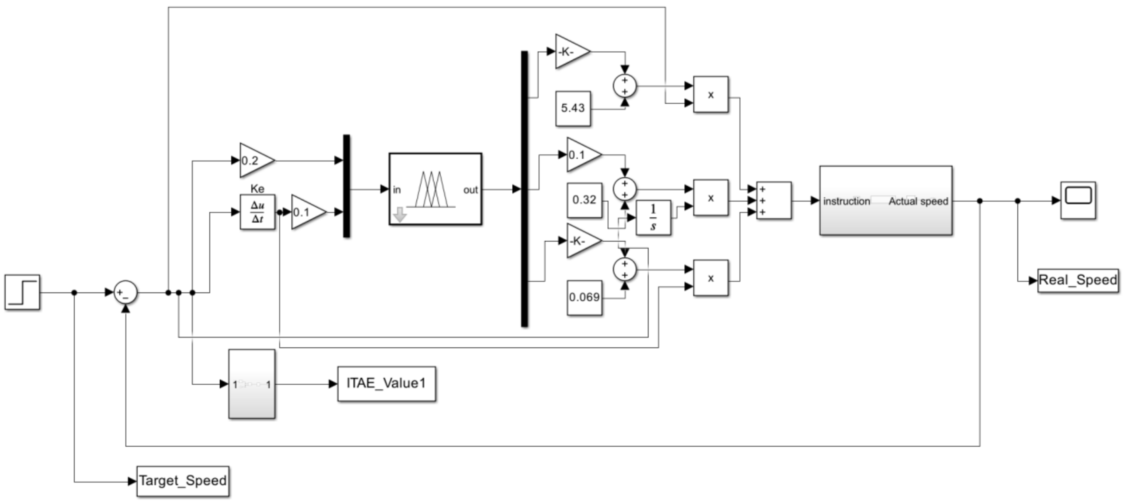

Fig. 5 - Architecture diagram of the fuzzy PID control system

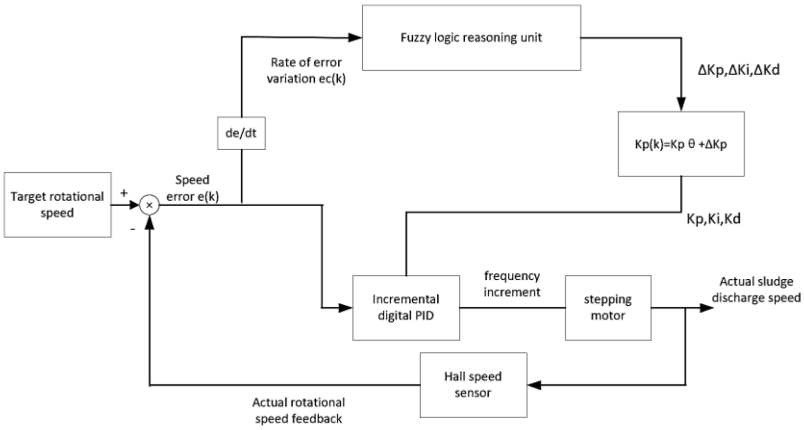

Fig. 6 - Fuzzy PID simulation model

Improvement of population initialization with tent mapping introduction

The standard WOA uses pseudo-random numbers to generate the initial population, which may cause individuals to cluster within the optimization space, thereby reducing the search efficiency of the algorithm in the early stage. The Tent mapping has a strict uniform probability density distribution and pure chaotic characteristics within the [0,1] interval. Its mathematical expression is:

$$z_{i+1} = z_i/\alpha, \quad 0 \le z_i < \alpha \tag{11}$$

$$z_{i+1}(1-z_i)/(1-\alpha), \quad \alpha \le z_i \le 1 \tag{12}$$

The value of α is set to the typical value of 0.499. A chaotic sequence is generated using the Tent mapping, and then it is transformed into the initial positions of the fuzzy PID parameters through the inverse mapping. This enables the initial population of pilot whales to evenly cover the entire parameter domain, thereby improving the global optimization starting point of the algorithm from the very beginning.

Nonlinear convergence factor strategy based on cosine function

The linearly decreasing approach results in less global exploration time in the initial stage of the algorithm, and too rapid attenuation in the local development stage later on, which makes it easy to miss the optimal solution. The actual parameter optimization process is a highly complex nonlinear dynamic process. Therefore, this paper proposes a nonlinear convergence factor update strategy based on the cosine function, and the mathematical model is modified as:

$$a = 2 \cdot \cos\left(\frac{\pi}{2} \cdot \frac{t}{T_{max}}\right) \tag{13}$$

The improved α value maintains a relatively slow decay rate in the early stage of iteration, providing the population with more ample time for global and extensive search, thus avoiding premature convergence of the algorithm. In the later stage of iteration, as the slope of the cosine function increases, the α value rapidly decays to 0, prompting the algorithm to converge quickly to the high-precision local extremum point.

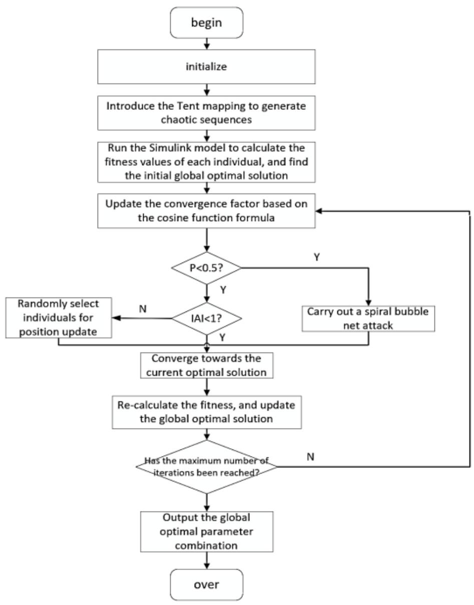

Fig. 7 - Fuzzy PID simulation model

Algorithm simulation analysis

A simulation model was built on the MATLAB/Simulink platform, and step response simulations were conducted for the traditional PID, basic fuzzy PID, and IWOA-fuzzy PID. The optimal physical operating range of the system is 10 to 60 r/min. Therefore, in this section, the target rotational speed command of the system is set to the median value within this range, which is 30 r/min.

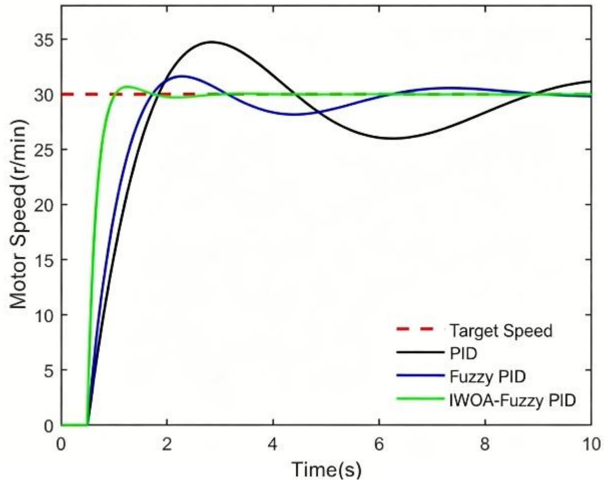

Fig. 8 - Fuzzy PID simulation model

Table 2

Comparison of step response performance indicators

Control algorithm	Rise time [s]	Overshoot [%]	Accommodation time[s]
PID	2.45	16.7	8.8
Fuzzy PID	1.68	6.7	6.02
IWOA - Fuzzy PID	0.92	3.3	1.55

In the PID algorithm, the initial parameters are K_p = 1.23, K_i = 0.84, and K_d = 0.05. Due to the presence of a 0.485-second pure lag in the motor speed response, the relatively large integral coefficient accumulated a huge error energy within the starting dead zone, resulting in a severe integral saturation phenomenon. The weak differential damping was unable to effectively restrain it, directly causing the response curve to soar to around 35 r/min, with a severe overshoot and long-term oscillation. In the fuzzy PID algorithm, the system introduced error and error rate change K_e = 0.2 and Kec = 0.1, and the three compensation quantities ΔK_p, ΔK_i, and ΔK_d were 0.57, 0.1, and 0.05 respectively. Due to the limitation of manual experience setting, the system could not fully exert its potential. Eventually, after 50 generations of deep evolution using the IWOA algorithm, the system successfully escaped from the local optimal trap and locked onto the global optimal parameters K_p = 5.43, K_i = 0.32, and K_d = 0.069. After generating only 1.8% overshoot and a brief real mechanical micro-vibration, it quickly stabilized and precisely matched the target rotational speed command of 30 r/min.

Calibration test of the relationship between fertilizer discharge amount and rotational speed

In this experiment, the calibration speed range of the fertilizer discharge shaft was set at 10 to 60 r/min, and the step size of the test speed was set at 10 r/min. All these were strictly repeated for 6 independent sampling measurements. When calculating the data later, the average values of each group were extracted as the actual fertilizer discharge amount at that speed.

Table 3

Test data on fertilizer discharge amount at different rotational speeds

Rotate speed [r/min]	Measure-ment 1 [g]	Measure-ment 2 [g]	Measure-ment3 [g]	Measure-ment 4 [g]	Measure-ment 5 [g]	Measure-Ment 6 [g]	Average fertilizer application rate [g/min]
10	1121.2	1135.4	1128.5	1119.8	1138.1	1129.2	1128.7
20	2650.3	2681.2	2658.5	2675.9	2645.1	2679.6	2665.1
30	3405.6	3448.2	3415.9	3438.1	3395.4	3454	3426.2
40	4610.2	4655.8	4625.5	4648.1	4602.4	4667.4	4634.9
50	5145.2	5205.6	5168.4	5192.1	5130.5	5219	5176.8
60	6250.5	6345.2	6280.4	6325.8	6240.1	6338.8	6296.8

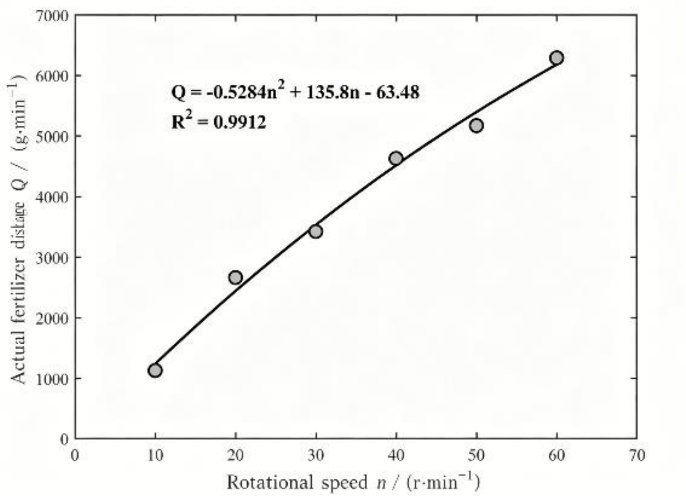

Fig. 9 - Speed and fertilizer discharge rate calibration curve

The coefficient of determination R^2 of the fitted equation is 0.9912. In the system's global closed-loop, this equation is used to convert the fertilizer application rate specified by the prescription map into a dynamic rotational speed executable by the hardware. After the controller obtains the local target displacement Q issued by the prescription chart, it needs to perform real-time reverse optimization calculation to convert it into the target rotational speed n_t of the stepper motor. The underlying control relationship is expressed as Eq. (14):

$$n_t = \frac{-135.8 + \sqrt{135.8^2 - 4 \times (-0.5284) \times (-63.48 - Q)}}{2 \times (-0.5284)} \tag{14}$$

Field trial

The experiment adopted the IWOA-fuzzy PID algorithm as the core driving strategy. The experiment was conducted at the Erliuhe Farm. The experimental equipment was a Jinjiang riding-type rice transplanting machine with a working width of 2.1 meters and equipped with a fan-type fertilizer distributor.

The test equipment includes an ESP32 microcontroller, a GNSS-RTK positioning receiver, a TB6600 stepper motor driver, a 24V power supply, a high-precision electronic balance, and a measuring tape.

The actual fertilizer discharge amount was measured using the box difference weighing method. Before starting the experiment, an adequate initial fertilizer mass W_1 was placed in the fertilizer box and weighed. After the transplanting machine completed the experiment, the remaining fertilizer mass W_2 in the box was weighed again. By calculating the difference between the two measurements ($\Delta W = W1 - W2$), the actual fertilizer discharge amount was obtained. The initial fertilizer mass in the box was 15 kg.

Fig. 10 - Field trial

The travel speed of the transplanting machine was fixed at 1 m/s. Six paths corresponding to different prescription grades were planned in the field, with each path having a length of 20 m. A fertilizer collection bag was attached to the fertilizer discharge outlet, and the fertilizer discharge system was started at the beginning of each path. The motor pulse signal was stopped at the end of the 20 m path. The remaining fertilizer mass in the fertilizer box was then weighed using an electronic balance. The actual fertilizer application rate was calculated using Eq. (15), and the relative error δ was calculated using Eq. (16):

$$M_a=\frac{10000\times m_a}{L\times W} \tag{15}$$

$$\delta=\frac{M_a\text{-}M_t}{M_t}\times 100\% \tag{16}$$

where:

M_a is the actual fertilizer application rate per unit area, (kg/hm²); m_a is the total mass of discharged fertilizer, (kg); L is the working length, (m); W is the working width, (m); δ is the fertilizer application error; M_t is the target fertilizer application rate, (kg/hm²).

RESULTS

The fertilizer mass measured for each prescription level was substituted into the formula for calculation, and the results of the constant-rate fertilizer application test are shown in Table 4.

Table 4

The results of the fertilizer application test

Prescription chart level	Target fertilizer application rate [kg/hm²]	Total discharged fertilizer mass [ma/kg]	Actual fertilizer application rate [kg/hm²]	Relative error [%]
1	273.94	1.167	277.86	1.43
2	287.54	1.176	280	-2.62
3	301.14	1.317	313.57	4.13
4	314.74	1.31	311.9	-0.9
5	328.34	1.409	335.48	2.17
6	342.49	1.384	329.52	-3.79

CONCLUSIONS

This study addressed the key challenges of fertilization operations in cold-region paddy fields and developed an intelligent variable-rate fertilization system driven by integrated prescription maps. Based on measured field soil data, the study completed the integration and rasterization of multiple nutrient prescriptions for nitrogen, phosphorus, and potassium, thereby solving the problem that traditional single-nutrient prescriptions cannot meet the coordinated fertilizer-supply requirements of rice cultivation. Based on the impeller-type fertilizer discharge device, a mechanism analysis was conducted, and a correlation model between fertilizer application rate and motor speed was established. In addition, a spatiotemporal delay compensation strategy was introduced to effectively correct fertilizer placement deviations caused by machine travel and fertilizer transport. The improved whale optimization algorithm was used to optimize the parameters of the fuzzy PID controller, significantly enhancing the dynamic control capability of the system. The test results showed a strong linear correlation between fertilizer application rate and motor speed, with a coefficient of determination of 0.9912. The optimized control algorithm achieved a step-response overshoot of 3.3% and a settling time of only 1.55 s, while the fertilizer application errors under different field operating conditions were controlled within ±5%, meeting the field agronomic requirements of rice cultivation.

ACKNOWLEDGEMENT

This research is funded by the following projects: the Jiansanjiang Rice Industry Research Institute Project（JCY202403）; the Special Project for Central Government to Guide Local Science and Technology Development（ZY20B05）.

REFERENCES

[1] Chen, L.P., Huang, W.Q., Meng, Z.J. (2008). Design of variable fertilization controller based on CAN bus (基于 CAN 总线的变量施肥控制器设计) [J]. *Journal of agricultural machinery science*, (08):101-104+185.

[2] Dong, S., Shu, X. D., Chung, G.B. (2020). Improved whale optimization algorithm based on the tent chaotic mapping and nonlinear convergence factor[J]. *Journal of physics: conference series*,1682(1):012055.
[3] Dou, H., Hu, L. (2026). Precision variable-rate fertilizer application method based on real-time field soil electrical conductivity sensing [J]. *Computers and Electronics in Agriculture*, 241111267-111267.
[4] Kun, H., Lian, Z., Ping, L. (2023). Side-Deep fertilization stabilizes double-cropping rice yield, increases N and P utilization, and reduces N and P losses [J]. *Land*, 12(3):724-724.
[5] Li, T., Li, J. (2024). Fuzzy PID control based on genetic algorithm optimization inverted pendulum system [J]. *Journal of Physics: Conference Series*, 2816(1):012001-012001.
[6] Li, Y. (2025). Research on variable sowing and fertilization control system - based on financial accounting precision (变量播种施肥控制系统的研究——基于财务会计精细化) [J]. *Agricultural mechanization research*, 46(02):216-220.
[7] Li, Z.P., Liang, C.Y., Li, P. (2022). *Research status and prospects of precision fertilization technology (精准施肥技术研究现状和展望)* [J]. *Tropical agricultural engineering*, 46(03):47-50.
[8] Liu, Y.C. (2012). *Research on key technologies for variable-fertilizer application and precision farming equipment* (变量配肥施肥精准作业装备关键技术研究) [D]. Chinese academy of agricultural mechanization sciences.
[9] Luo, L., Zhang, F.G., Li, Y.T. (2018). Research on variable fertilization control system without GPS positioning (基于无 GPS 定位的变量施肥控制系统的研究) [J]. *Agricultural mechanization research*, 40(01):96-100.
[10] Ma, X., Zhao, X., Liu, S.S. (2023). Design and experiment of variable fertilizer application device for solid particles fertilizer in high-speed rice transplanter (水稻高速插秧机固体颗粒肥料变量施肥装置设计与试验) [J]. *Journal of agricultural machinery science*, 54(09):99-110
[11] Mou, G.T., Feng, Y.J., Li, J. (2017). *Research on recommended fertilizer amount for rice in mountain villages based on GIS (基于 GIS 的山地村域水稻推荐施肥量研究)* [J]. *Chinese rice*, 23(04):119-122.
[12] Qi, W.Z., Wang, J.X., Liu, S.X. (2019). Design and experiment of the variable fertilizer application system for rice and wheat machines (稻麦变量施肥机控制系统设计与试验) [J]. *Agricultural mechanization research*, 41(08):72-79.
[13] Xu, Y., Jin, Y., Sun, Z. (2025). PSO-Based System Identification and Fuzzy-PID Control for EC Real-Time Regulation in Fertilizer Mixing System[J]. *Agronomy*, 15(5):1259-1259.
[14] Wang, B.W. (2024). *Design and experimental research of impeller-type sub-surface fertilization device for rice (叶轮式水稻侧深施肥装置设计与试验研究)* [D]. Heilongjiang Bayi Agricultural University.
[15] Wang, J.F., Lv, Z.Y., Zhao, M.Y. (2024). Design and experiment of a variable fertilizer application system for rice based on prescription maps (基于处方图的水稻侧深变量施肥控制系统设计与试验) [J]. *Journal of agricultural machinery science*, 55(09):151-162.
[16] Wang, N., Zhuang, W.D. (2024). Research status and development suggestions of variable fertilization technology (变量施肥技术的研究现状与发展建议) [J]. *Modernized agriculture*, 03:77-79.
[17] Wang, Z.Y., Wang, L. (2025). Multi-strategy improved whale optimization algorithm and its applications(多策略改进的鲸鱼优化算法及其应用) [J]. Journal of Harbin Engineering university, 46(05):997-1004.
[18] Zhou, C., Liu, K., Yao L.L. (2025). Research status and prospects of key technologies for prescription-type variable fertilization (处方图变量施肥关键技术研究现状与展望) [J]. *Chinese journal of agricultural machinery chemistry*, 46(08):238-245.